EJNMMI RESEARCH

ORIGINAL RESEARCH

Open Access

Evaluation of the theranostic potential of [^{64}Cu]$CuCl_2$ in glioblastoma spheroids

Catarina I. G. Pinto[1], André D. M. Branco[2], Sara Bucar[2], Alexandra Fonseca[3,4], Antero J. Abrunhosa[3,4], Cláudia L. da Silva[2], Joana F. Guerreiro[1,5] and Filipa Mendes[1,6*]

Abstract

Background Glioblastoma is an extremely aggressive malignant tumor with a very poor prognosis. Due to the increased proliferation rate of glioblastoma, there is the development of hypoxic regions, characterized by an increased concentration of copper (Cu). Considering this, ^{64}Cu has attracted attention as a possible theranostic radionuclide for glioblastoma. In particular, [^{64}Cu]$CuCl_2$ accumulates in glioblastoma, being considered a suitable agent for positron emission tomography. Here, we explore further the theranostic potential of [^{64}Cu]$CuCl_2$, by studying its therapeutic effects in advanced three-dimensional glioblastoma cellular models. First, we established spheroids from three glioblastoma (T98G, U373, and U87) and a non-tumoral astrocytic cell line. Then, we evaluated the therapeutic responses of spheroids to [^{64}Cu]$CuCl_2$ exposure by analyzing spheroids' growth, viability, and cells' proliferative capacity. Afterward, we studied possible mechanisms responsible for the therapeutic outcomes, including the uptake of ^{64}Cu, the expression levels of a copper transporter (CTR1), the presence of a cancer stem cell population, and the production of reactive oxygen species (ROS).

Results Results revealed that [^{64}Cu]$CuCl_2$ is able to significantly reduce spheroids' growth and viability, while also affecting cells' proliferation capacity. The uptake of ^{64}Cu, the presence of cancer stem-like cells and the production of ROS were in accordance with the therapeutic response. However, expression levels of CTR1 were not in agreement with uptake levels, revealing that other mechanisms could be involved in the uptake of ^{64}Cu.

Conclusions Overall, our results further support [^{64}Cu]$CuCl_2$ potential as a theranostic agent for glioblastoma, unveiling potential mechanisms that could be involved in the therapeutic response.

Keywords Copper-64 chloride, Theranostics, Radiobiology, Glioblastoma, Spheroids

*Correspondence:
Filipa Mendes
fmendes@ctn.tecnico.ulisboa.pt
[1] C2TN – Centro de Ciências e Tecnologias Nucleares, Instituto Superior Técnico, Universidade de Lisboa, Lisbon, Portugal
[2] Department of Bioengineering, iBB - Institute for Bioengineering and Biosciences, Associate Laboratory i4HB - Institute for Health and Bioeconomy, Instituto Superior Técnico, Universidade de Lisboa, Lisbon, Portugal
[3] CIBIT/ICNAS Instituto de Ciências Nucleares Aplicadas à Saúde, Universidade de Coimbra, Coimbra, Portugal
[4] ICNAS PHARMA, Universidade de Coimbra, Coimbra, Portugal
[5] Present Address: CIISA - Centro de Investigação Interdisciplinar em Sanidade Animal, Faculdade de Medicina Veterinária, Universidade de Lisboa and Laboratório Associado Para Ciência Animal e Veterinária (AL4AnimalS), Lisbon, Portugal
[6] DECN – Departamento de Engenharia e Ciências Nucleares, Instituto Superior Técnico, Universidade de Lisboa, Lisbon, Portugal

Background

Glioblastoma is the most common primary brain cancer in adults, arising within the central nervous system. It belongs to a heterogeneous family of brain tumors known as gliomas, which derive from glial cells or their precursors [1].

Glioblastoma is classified as a grade IV tumor by the World Health Organization (WHO), being a highly aggressive subtype of glioma with high rates of cell division, abnormal blood vessel growth and central necrotic areas [1]. It is considered incurable, having a very poor median survival of only 14–16 months, even following the combination of several therapeutic strategies including surgical resection, adjuvant radiation therapy (RT) and temozolomide (TMZ) treatment [2].

Additionally, glioblastoma is known to have increased cell proliferation associated with an erratic tumor neovascularization that leads to poor oxygen diffusion, and thus hypoxia [3]. The occurrence of hypoxic regions (< 2% O_2) leads to the secretion of vascular endothelial growth factor, and, consequently, to angiogenesis, increasing the concentration of several signaling factors in these areas, including copper (Cu) [4]. Indeed, Turecký and colleagues have shown that serum concentrations of Cu were significantly higher in patients with brain tumors than in healthy subjects, being even more increased in patients with more malignant tumors, such as glioblastoma [5].

Copper is a transition metal that is the main building block in more than 30 metalloenzymes and takes part in angiogenesis, a vital process for tumor progression [6]. Furthermore, it alternates between two oxidation states, Cu^{+} and Cu^{2+}, generating reactive oxygen species (ROS). When ROS are in excess, these can induce cancer cell cycle arrest, senescence, and apoptosis [4, 7].

Chemically, Cu offers a wide variety of isotopes, such as ^{61}Cu, ^{62}Cu, ^{64}Cu, and ^{67}Cu, which can be incorporated in radiopharmaceuticals, being useful for nuclear medicine. Among the isotopes, ^{64}Cu has attracted more interest due to its advantageous characteristics [8]. Specifically, ^{64}Cu isotope decays to ^{64}Zn by β^{-} (electron) emission, or to ^{64}Ni by β^{+} (positron) emission or electron capture, which stimulates the emission of Auger electrons [9]. This means that ^{64}Cu, a theranostic radioisotope, has the potential to be used for diagnostic purposes, as a Positron Emission Tomography (PET) tracer, and for therapeutic purposes, due to the emission of both β^{-} particles and Auger electrons [10].

^{64}Cu labeled diacetyl-2,3-bis(N4-methyl-3-thiosemicarbazone) ([^{64}Cu]Cu-ATSM) is a probe that has been successfully used for PET imaging of hypoxic regions of tumors in humans, including glioblastoma [11, 12]. Evidence suggests that high uptake of [^{64}Cu]Cu-ATSM correlates with the treatment response and poor prognosis [13]. Additionally, Pérès and colleagues have shown that both [^{64}Cu]Cu-ATSM and [^{64}Cu]$CuCl_2$ accumulate in glioblastoma tumors, not only in hypoxic areas but also in invasive areas closer to the tumor periphery [14]. [^{64}Cu]$CuCl_2$ is the simplest chemical form of ^{64}Cu, being easily available, highly stable, and not requiring complexation with targeting [9, 15].

Both ^{64}Cu-based molecules, [^{64}Cu]Cu-ATSM and [^{64}Cu]$CuCl_2$, have been shown to be strongly retained in hypoxic cells of glioblastoma. These are also associated with increased expression of Cu transporters, not only in hypoxic cells but also in non-hypoxic cells [14].

Clinical studies have reported a selective accumulation of [^{64}Cu]$CuCl_2$ in glioblastoma (within 1 h after intravenous injection) with no adverse or clinically detectable pharmacological effects, supporting the potential of [^{64}Cu]$CuCl_2$ as a PET imaging agent [16]. Therapeutically, preclinical studies using xenografts of glioblastoma cells implanted in mouse models have shown that administration of a therapeutic dose of [^{64}Cu]$CuCl_2$ led to a significant tumor decrease (in some cases, complete tumor regression), with a concomitant survival rate increase in treated mice [9].

In the present work, we explored further the potential of [^{64}Cu]$CuCl_2$ as a theranostic agent for glioblastoma, making use of advanced culture systems, namely multicellular tumor spheroids. Spheroids are a three-dimensional (3D) culture system that can better replicate the in vivo environment of tumor cells. Through the promotion of cell-to-cell and cell-to-extracellular matrix (ECM) interactions, spheroids can re-establish the morphological, functional, and mass-transport properties observed in in vivo tumors [17]. Furthermore, advanced culture models, such as spheroids, are known to replicate the existence of a cancer stem cell (CSC) population that is able to self-renew and differentiate. CSCs are reported to be resistant to conventional chemotherapy and/or radiation therapy, playing an important role in cancer relapse and metastasis formation [15]. The aim of our work was to assess the therapeutic effect of [^{64}Cu]$CuCl_2$ on growth, viability, and survival capacity of glioblastoma spheroids while trying to elucidate some of the cellular mechanisms involved.

Methods

Cell lines and media

Human glioblastoma cell lines T98G and U87 were obtained from the America Type Culture Collection, while U373 was obtained from the European Collection of Authenticated Cell Cultures. Rat Astrocytes (RA) were obtained from Cell Applications, Inc.. T98G and U87

cell lines were cultured in Minimum Essential Medium (MEM) with GlutaMAX™ (Gibco, Thermo Fisher Scientific) supplemented with 10% fetal bovine serum (FBS) (Gibco, Thermo Fisher Scientific). U373 cell line was cultured in the same culture medium further supplemented with 1% non-essential amino acids (Gibco, Thermo Fisher Scientific) and 1% sodium pyruvate (Gibco, Thermo Fisher Scientific). RA cell line was cultured in RA growth medium (Cell Applications, Inc.). All cell lines were grown at 37 °C in a humidified atmosphere of 5% CO_2 and tested for mycoplasma using the LookOut® mycoplasma Polymerase Chain Reaction (PCR) Detection kit (Sigma-Aldrich, Merk).

Spheroid culture

Cells were cultured on T25 or T75 culture flasks (Thermo Fisher Scientific). After reaching 80–90% confluence, cell suspensions with the desired cell density were prepared. Two hundred µl of each cell suspension were seeded on Nunclon™ Sphera™ ultra-low attachment 96-well plates (Thermo Fisher Scientific). Cell density per well was 4000, 2000, 1250, and 7000 for T98G, U373, U87, and RA cell lines, respectively. Plates were centrifuged at 405 g for 5 min and incubated at 37 °C in a humidified atmosphere of 5% CO_2.

[^{64}Cu]$CuCl_2$ solution preparation

^{64}Cu was produced by irradiation of a ^{64}Ni target in a medical cyclotron as previously described [18, 19] and supplied as a solution of [^{64}Cu]$CuCl_2$ in 0.1 M HCl. Prior to the biological studies, the pH of the solution was adjusted to ~ 7 by adding appropriate volumes of sterile 0.1 M phosphate buffer pH 7.2.

Spheroids' viability, growth, and circularity determination

Three-day-old spheroids were exposed to 0.56, 1.11, and 2.76 MBq of [^{64}Cu]$CuCl_2$, by incubation with the [^{64}Cu]$CuCl_2$ solutions prepared in culture medium and grown for 8 additional days. In the control condition, spheroids were incubated with regular culture medium (0 MBq). Four days after exposure to [^{64}Cu]$CuCl_2$, half of the exhausted medium was replaced by fresh culture medium, and on the 8th day following exposure, the viability of the spheroids was evaluated using the acid phosphatase (APH) assay, as previously described [15]. Two to four independent assays were performed.

Spheroid growth was monitored over the culture period using a Primovert Inverted ZEISS Microscope, under a total magnification of 40×, with an integrated HDcam camera and using the ZEN 3.5 (blue edition) software. The spheroid area was measured using the software SpheroidSizer [20], and the circularity was calculated according to [1].

$$\text{Circularity} = (4\pi \times \text{Area})/\text{Perimeter}^2 \quad (1)$$

Colony formation assay

As described above, three-day-old spheroids were exposed to 0.56 and 2.76 MBq of [^{64}Cu]$CuCl_2$. In the control condition, spheroids were incubated with regular culture medium (0 MBq). After 3 h of exposure, three spheroids per condition were pooled in a microtube, spun down, and the supernatant was discarded. Spheroids were then washed with 500 µl of phosphate saline buffer (PBS) and incubated with 1X TrypLE (Gibco, Thermo Fisher Scientific) at 37 °C for 5 min. Dissociated cells were counted and seeded in 6-well plates (Thermo Fisher Scientific). For T98G and U373 cell lines, 200 cells were seeded for the control conditions and 600 cells for [^{64}Cu]$CuCl_2$-exposed cells. For the remaining U87 and RA cell lines, 400 cells were seeded for the control conditions and 800 cells for [^{64}Cu]$CuCl_2$-exposed cells. After an incubation period of 14 days at 37 °C, cells were fixed with a solution of 3:1 methanol:acetic acid (Carlo Erba Reagents and PanReac Quimica CA) at − 20 °C for 20 min. Following washing, fixed cells were stained with 4% Giemsa (Sigma-Aldrich, Merk) in PBS for 10 min. Colonies with more than 50 cells were counted. Results are expressed as the fraction of cellular survival upon treatment compared to the untreated control. Three to five independent assays were performed.

[^{64}Cu]$CuCl_2$ cellular uptake assay

Cellular uptake studies were performed with three-day-old spheroids. A volume of 100 µl of culture medium was removed from each well, and 100 µl of 0.93 MBq/ml of [^{64}Cu]$CuCl_2$ in culture medium was added to the spheroids. Spheroids were incubated for 1, 2, and 3 h, at 37 °C. At every time point, 7 spheroids of each cell line were pooled in a microtube, spun down, and the supernatant was removed. Spheroids were then washed with 500 µl of PBS and lysed with 500 µl of 1 M NaOH solution, at 37 °C for 10 min. Radioactivity present in lysed cells was measured using a Hidex AMG Automatic Gamma Counter. The uptake was calculated as the percentage of total activity normalized to spheroid mean area of each cell line and to the uptake of U87 spheroids measured at 1 h. Three to five independent assays were performed.

Protein extraction and western blot analysis

To determine the basal expression of copper transporter 1 (CTR1), 24 three-day-old spheroids of each cell line were collected and lysed in ice-cold CelLytic™ M Cell Lysis reagent (Sigma-Aldrich, Saint Louis, MO, USA), containing a cocktail of protease inhibitors (Roche

Applied Science, Penzberg, Germany). Cellular suspensions were centrifuged at 15,000 g for 15 min and the resultant supernatant was collected. Protein concentration was determined using the DC™ Protein Assay (Biorad, Hercules, CA, USA).

Western blot analysis was performed as previously described [21].

Immunophenotypic characterization

Immunophenotypic characterization was performed on cells harvested from spheroids. Three-day-old spheroids of each tumor cell line were pooled together and dissociated with Tryple. After washing with PBS, cells were resuspended in FACS buffer (PBS supplemented with 2% FBS) and distributed at a density of approximately 1×10^5 cells/tube. Cells were first incubated with Far Red LIVE/DEAD Fixable Dead Cell Stain Kit (Thermo Fisher Scientific), according to the manufacturer's instructions, to assess cell viability. Following a washing step with FACS buffer, cells were incubated with CD44 PE (clone BJ18, Biolegend) or CD117 PE (clone 104D2, Biolegend) anti-human antibodies, at room temperature for 15 min. After washing, cells were fixed with 100 µl of 2% formaldehyde at 4 °C for 15 min, washed, and resuspended in Fluorescence-Activated Cell Sorting (FACS) buffer. Cells were acquired on a FACSCalibur flow cytometer (BD Biosciences) and data was analyzed using FlowJo v10 software (FlowJo LLC).

ROS determination

To evaluate the production of ROS after exposure to [^{64}Cu]$CuCl_2$, three-day-old spheroids were pre-incubated with Fluorobrite™ Dulbecco's modified eagle's medium (DMEM) (Gibco®, Waltham, MA, USA) containing 20 µM 2,7-dichlorodihydrofluorescein diacetate (H_2DCF-DA) (Invitrogen, Thermo Fisher Scientific) for 1 h at 37 °C. H_2DCF-DA is a fluorogenic dye (capable of cell membrane permeability) that is converted into 2,7-dichlorodihydrofluorescein (DCF), in the presence of ROS. After incubation, the probe that did not enter cells was discarded and spheroids were then exposed to 0.56, 1.11, and 2.76 MBq of $^{64}CuCl_2$. The fluorescent signal of DCF was measured at specific timepoints, using a Varioskan Lux multimode microplate reader (ThermoFisher Scientific, Waltham, MA, USA), at 492 nm excitation and 517 nm emission. The signal of blank wells (with no cells) was subtracted from spheroids' fluorescence signals obtained and the results were expressed as the fold change to the control condition (no exposure to [^{64}Cu]$CuCl_2$). Two to three independent assays were performed.

Statistical analysis

GraphPad Prism 9 software was used to perform statistical analysis. Data are shown as mean values ± standard error of the mean (S.E.M.). Statistically significant differences were evaluated considering a threshold of p-value = 0.05. One-way analysis of variance (ANOVA), followed by Dunnett's test, was used to determine differences between groups under study.

Results

Effects of [^{64}Cu]$CuCl_2$ exposure on the growth of glioblastoma spheroids

Three glioblastoma cell lines were selected to establish spheroids, including two cell lines that are known to be tumorigenic in nude mice, U373 and U87, and a non-tumorigenic line, T98G. RA were used as a non-tumoral control. All the cell lines were able to form compact cell aggregates with a spherical form (Additional file 1: Fig. S1). Spheroids derived from the U87 cell line were the only ones that grew in size throughout the eleven-day culture period. On the other hand, spheroids derived from the other cell lines decreased in size in the initial 4 days and then their mean area stabilized throughout the culture period. On the third day of culture, all spheroids were completely formed, with a compact appearance and a mean diameter ranging from 350 to 450 µm. Considering this, the third day of culture was chosen to start all studies performed in the following sections.

First, as an initial approach to evaluate the potential therapeutic effect of [^{64}Cu]$CuCl_2$ on glioblastoma spheroids, we tested if spheroids' growth was affected by exposure to different doses of ^{64}Cu. The results obtained revealed that the three cell lines tested had different behaviors after exposure to the radionuclide (Fig. 1). Interestingly, only one of the glioblastoma cell lines—U87—displayed a statistically significant reduction in growth when compared to the non-exposed control (Fig. 1A). In U87 spheroids, growth impairment was independent of the ^{64}Cu dose to which spheroids were exposed, being observed after more than 24 h of exposure. On the other hand, spheroids derived from U373 and T98G exhibited no significant changes in their growth behavior when exposed to [^{64}Cu]$CuCl_2$, in comparison to control conditions (Fig. 1B, C). Nonetheless, the presence of small cellular debris surrounding the spheroids was detectable for all glioblastoma spheroids exposed to the ^{64}Cu. This could possibly be the result of partial spheroid disaggregation and cell death, suggesting that ^{64}Cu exposure affected spheroids' integrity. In the case of spheroids derived from the non-tumoral cell line (Fig. 1D), exposure to the radioactive compound led to a small decrease in their growth, suggesting that non-tumoral cells can also be damaged by [^{64}Cu]$CuCl_2$.

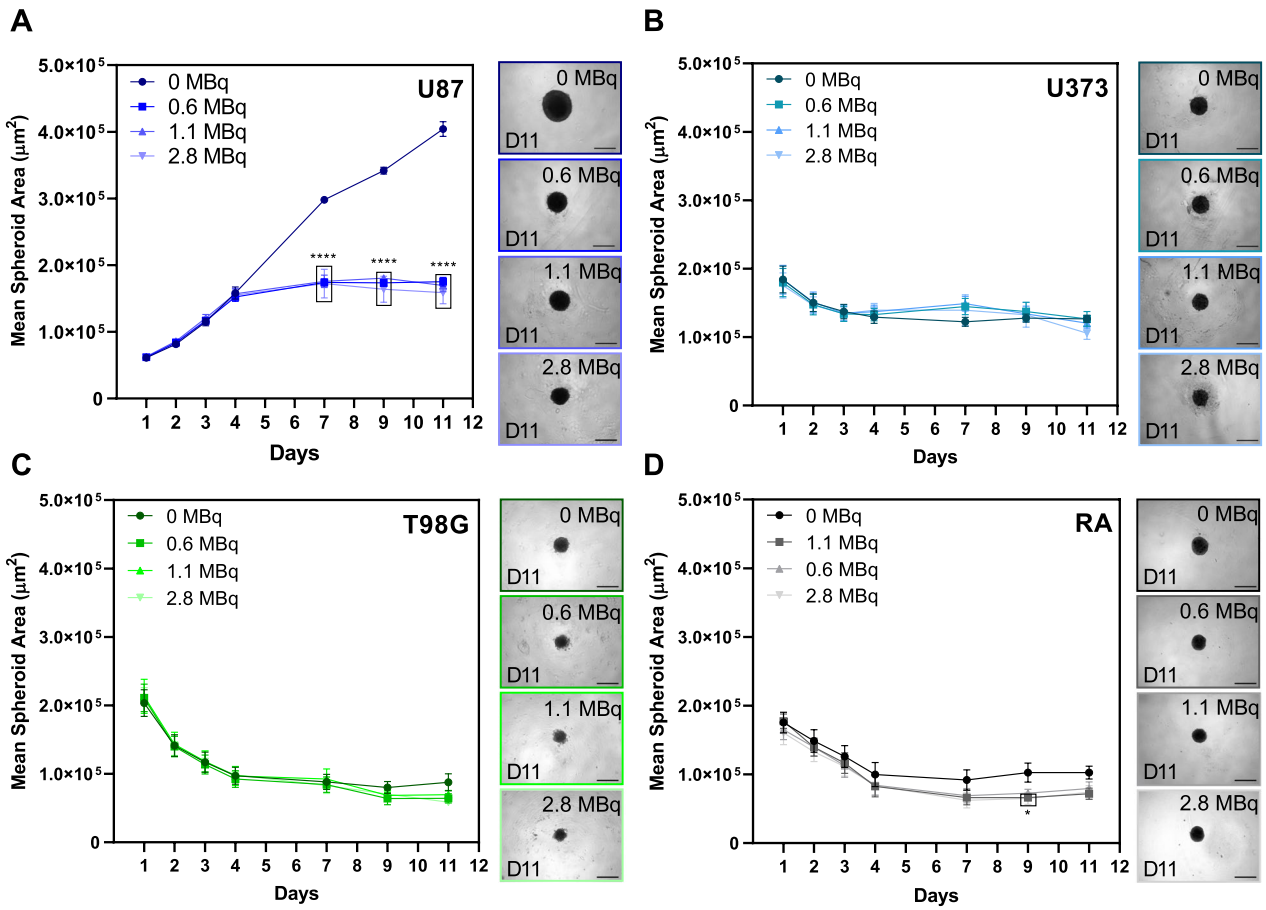

Fig. 1 Effects of [^{64}Cu]$CuCl_2$ exposure on three-day old spheroids. **A–D** Representative microscope images of eleven-day old spheroids exposed to 0, 0.6, 1.1, and 2.8 MBq. Growth curves represented by the mean spheroid area (µm^2) of U87, U373, T98G, and RA spheroids, respectively, as a function of the number of days in culture are also shown. Scale bar: 500 µm. Data are presented as mean values ± S.E.M. of 2 to 4 independent assays. *$p < 0.05$, ****$p < 0.0001$

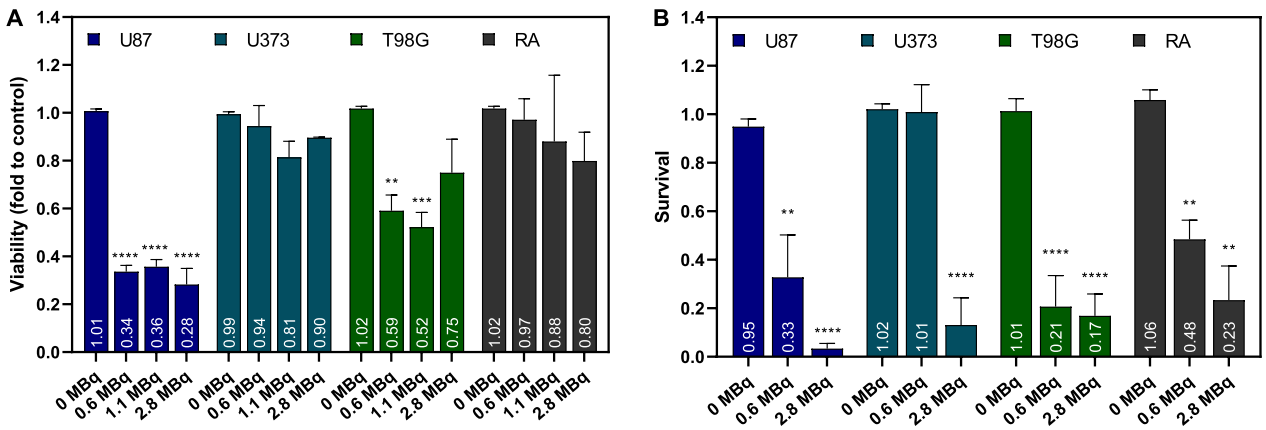

Fig. 2 **A** Viability of spheroids derived from U87, U373, T98G, and RA cell lines, evaluated after eight days of [^{64}Cu]$CuCl_2$ exposure, using the APH assay. Results are presented as the fold change to each cell line's respective untreated control. Data are presented as mean values ± S.E.M. of 2 to 4 independent assays. **B** Survival fraction of spheroid-derived cells from U87, U373, T98G, and RA cell lines after 3 h of [^{64}Cu]$CuCl_2$ exposure, presented as a fraction of the untreated control, determined through the clonogenic assay. Data are presented as mean values ± S.E.M of 3 to 5 independent assays. **$p < 0.01$, ***$p < 0.001$, ****$p < 0.0001$

To further study the damage caused by ^{64}Cu exposure, spheroids' circularity was evaluated (Additional file 1: Fig. S2). While exposure to ^{64}Cu led to small changes in their circularity, particularly in the case of U87 and RA spheroids (Additional file 1: Fig. S2A and D, respectively), circularity values remained very close to 1, meaning that all spheroids presented a circular shape throughout time.

Effects of [^{64}Cu]$CuCl_2$ exposure on spheroids' viability and the clonogenic capacity of spheroid-derived cells

To further study the effects of [^{64}Cu]$CuCl_2$ exposure on glioblastoma spheroids, we evaluated their viability. Spheroid viability was determined eight days after [^{64}Cu]$CuCl_2$ exposure, using the APH assay (Fig. 2A). In agreement with the abovementioned results, the viability of U87 spheroids was severely affected by exposure to [^{64}Cu]$CuCl_2$. The decrease in viability (of about 60%) was independent of the dose to which spheroids were exposed. The viability of T98G spheroids was also affected after exposure to [^{64}Cu]$CuCl_2$, leading to, approximately, a 40% decrease when spheroids were incubated with 0.6 and 1.1 MBq. In the case of U373 and RA spheroids, our results revealed that their viability was less affected by exposure to the radionuclide, suggesting an increased resistance of both cell lines to the treatment.

Assessment of the survival fraction using the clonogenic assay is an established standard assay to determine cell radiosensitivity. Thus, we performed a clonogenic assay to assess the proliferation capacity of cells derived from three-day-old spheroids that were exposed to ^{64}Cu for 3 h (Fig. 2B). For cells derived from U87 spheroids, results showed that [^{64}Cu]$CuCl_2$ exposure affected their proliferative capacity, in comparison to the untreated control condition, demonstrating a high sensitivity towards ^{64}Cu exposure. In particular, a correlation was shown between the dose to which spheroids were exposed and the extent to which cell clonogenic capacity was affected. Similarly to U87 cells, T98G cells derived from spheroids exposed to [^{64}Cu]$CuCl_2$ also had their proliferative capacity severely impaired, in comparison to the untreated control condition. Interestingly, the clonogenic ability of U373 cells was only affected when spheroids were exposed to the highest dose, highlighting an increased resistance to [^{64}Cu]$CuCl_2$ exposure at lower doses, unlike the other tumor cell lines. In what concerns the non-tumoral cells, RA, it was possible to see that their proliferative capacity was affected by [^{64}Cu]$CuCl_2$ exposure. Nonetheless, it is important to notice that from all cell lines exposed to the highest dose, RA cells were the ones with the highest survival fraction.

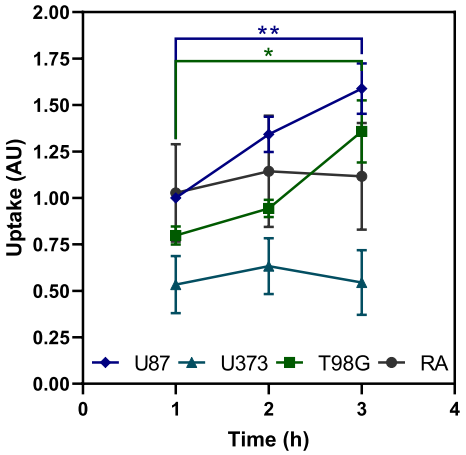

Fig. 3 Cellular uptake of [^{64}Cu]$CuCl_2$ in spheroids derived from glioblastoma and astrocyte cell lines. Cellular uptake was measured at 1, 2, and 3 h after incubation with 0.09 MBq of [^{64}Cu]$CuCl_2$. Uptake values were normalized to the spheroids' mean area of each cell line and the maximum uptake measured at 1 h in U87 spheroids. Data are presented as mean values ± S.E.M. of 3 to 5 independent assays. *$p < 0.05$, **$p < 0.01$

Cellular uptake of [^{64}Cu]$CuCl_2$ in glioblastoma spheroids

After assessing the possible therapeutic potential of [^{64}Cu]$CuCl_2$, we proceeded with mechanistic assays in an attempt to explain the effects observed. As a first approach, studies of cellular uptake were performed with spheroids from all cell lines (Fig. 3), to examine if the damages caused in spheroids could be related with [^{64}Cu]$CuCl_2$ presence in the cells. Spheroids derived from U87 had the highest uptake, showing increasing values throughout the exposure period. These results further support the abovementioned results of decreased spheroid growth, viability, and proliferative capacity. An identical uptake behavior was seen for T98G spheroids. On the other hand, spheroids derived from U373 had the lowest [^{64}Cu]$CuCl_2$ uptake throughout the time points. A stable uptake profile was maintained, which can also be associated with the previously observed spheroids' increased resistance. Spheroids derived from the non-tumoral cell line, RA, had the second highest uptake at the two initial time points but maintained a stable uptake profile throughout time.

Expression of the copper transporter CTR1 in glioblastoma spheroids

We also studied protein expression of one of the transporters responsible for Cu uptake, CTR1, by western blot analysis (Fig. 4 and Additional file 1: Fig. S3). Higher levels of expression of CTR1 were seen in glioblastoma spheroids, in comparison to the non-tumoral cell line,

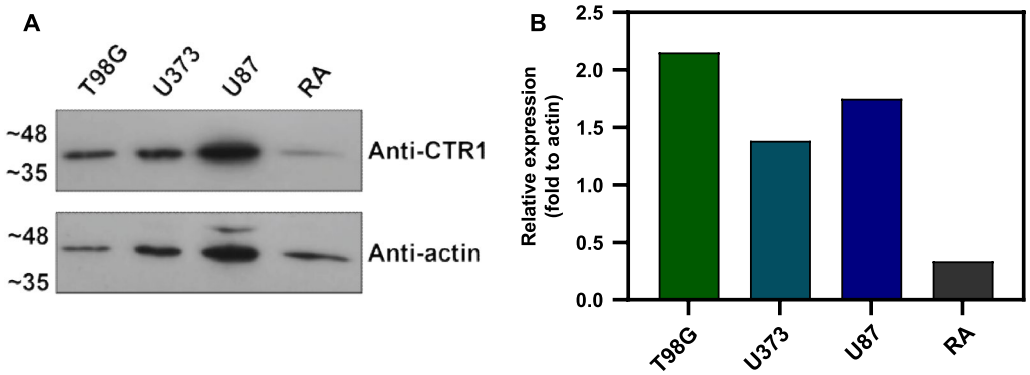

Fig. 4 Expression of the copper transporter, CTR1, in T98G, U373, U87 and RA spheroids. **A** Western blot analysis performed to study basal expression levels of CTR1 in spheroids derived from the panel of cell lines selected. Actin was used as a loading control, and detected after stripping of the membrane. **B** Quantification of CTR1 relative expression in comparison to actin expression

suggesting that ^{64}Cu uptake in RA spheroids might be due to alternative mechanisms. Interestingly, among the glioblastoma cell lines, U373 had the lowest expression of CTR1, which might partially explain why spheroids from this cell line had the lowest ^{64}Cu uptake under the conditions of our study.

Expression of cancer stem-like cell markers in glioblastoma spheroids

To further understand the underlying mechanisms involved in the therapeutic response of glioblastoma spheroids to [^{64}Cu]$CuCl_2$, we tried to evaluate the possible existence of a CSC population in spheroids. We performed an immunophenotypic characterization, through flow cytometry (Additional file 1: Fig. S4), to evaluate the expression of two surface markers commonly used to characterize the CSC population in glioblastoma, CD44 and CD117 [22, 23]. A clear difference between CD44 and CD117 expression was observed for the three glioblastoma cell lines (Fig. 5). Specifically, nearly all cells in spheroids, derived from every cell line tested, expressed CD44, while expression of CD117 was neglectable in U87 and U373 spheroids. Remarkably, spheroids derived from T98G had a small population of CD117$^+$ cells.

Evaluation of ROS production in glioblastoma spheroids exposed to [^{64}Cu]$CuCl_2$

Ionizing radiation, such as the one resulting from ^{64}Cu decay, is known to directly interact with water, generating ROS that can cause cellular damage, ultimately leading to apoptosis. Considering this known effect, we tried to understand if the damage caused in spheroids by [^{64}Cu]$CuCl_2$ was related to ROS production. The results obtained (Fig. 6) unveiled that exposure to high doses of [^{64}Cu]$CuCl_2$ triggered increased generation of ROS in spheroids derived from the U87 cell line. Interestingly, ROS production was not significantly increased in the other cell lines exposed to [^{64}Cu]$CuCl_2$.

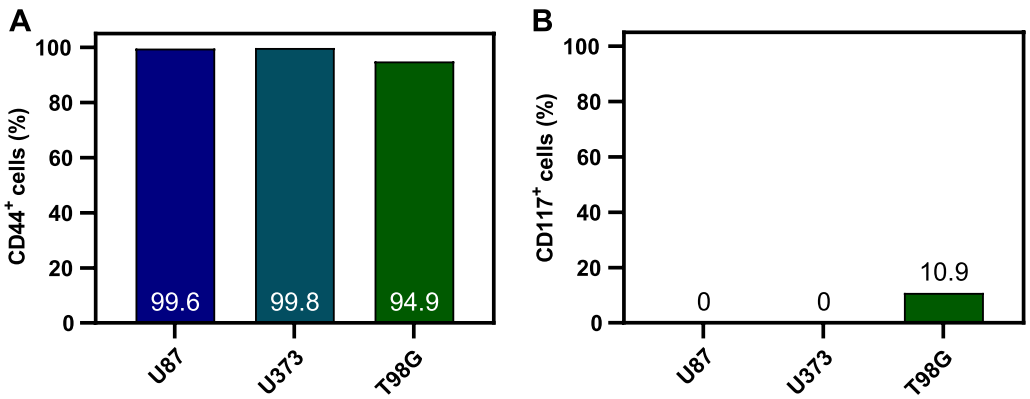

Fig. 5 Expression of **A** CD44 and **B** CD117 in three-day old spheroids derived from U87, U373, and T98G cell lines, gated on live cells

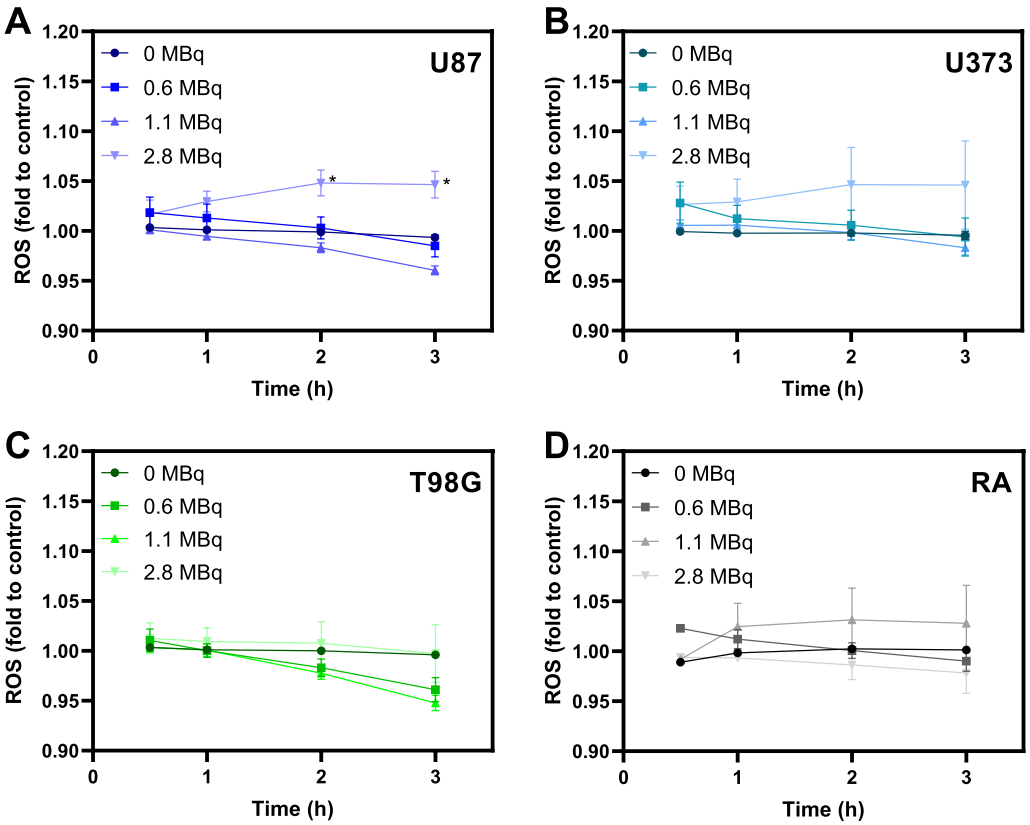

Fig. 6 Evaluation of ROS production on three-day old spheroids after exposure to different doses of [^{64}Cu]$CuCl_2$, probed with H_2DCFDA. **A–D** ROS production by U87, U373, T98G, and RA spheroids, respectively, using the H_2DCFDA method based on the detection of DCF fluorescence. Results are presented as the fold change to each cell line's respective untreated control at 1 h as a function of the time of exposure. Data are presented as mean values ± S.E.M. of 2–3 independent assays. *$p < 0.05$

Discussion

The use of [^{64}Cu]$CuCl_2$ for glioblastoma has been gathering interest among the scientific and medical communities in recent years. Several interesting studies were conducted not only in animal models but also in humans. Most of these studies were focused on the application of this radiopharmaceutical for glioblastoma diagnosis [16, 14]. Nonetheless, despite the recent advances, there are still some pitfalls in the knowledge acquired concerning the mode of action of [^{64}Cu]$CuCl_2$, mainly when the target application is therapy. To better understand the cellular and molecular mechanisms underlying the action of this compound, we studied the theranostic potential of [^{64}Cu]$CuCl_2$ for glioblastoma in 3D culture models, namely spheroids. These are a robust alternative to performing cellular studies prior to using animal models, having a much higher predictive value than monolayer cultures, which were once the go-to models for these types of studies [24].

Initially, spheroids were successfully established for all lines selected. These were completely formed by the third day of culture, with a mean diameter ranging from 350 to 450 µm. According to simulations, this size range allows for the establishment of a hypoxic core in spheroids, while avoiding the development of a necrotic core [24, 25]. The presence of a hypoxic core, in which cells are oxygen and nutrient-deprived, is an important characteristic of in vivo tumors that favors angiogenesis. Furthermore, hypoxia (< 2% O_2) has also been related to enhanced cell invasion capacity, development of metastasis, as well as tumor progression and subsequent increased resistance to treatment [26]. On the other hand, in our case, the presence of a necrotic core (in which cells die due to starvation) is undesirable, considering that it might interfere with [^{64}Cu]$CuCl_2$ cytotoxic evaluation [27].

We then aimed at assessing if exposure to the radionuclide would affect spheroids, not only in terms of growth but also their viability and proliferation capacity. In parallel, these studies were also conducted in a non-tumoral cell line derived from astrocytes, in an attempt to determine if there was a contrast in the response to ^{64}Cu-exposure between tumoral and non-tumoral cells found in the same environment. This

is particularly relevant in the case of this compound since the emission of β^- particles and Auger Electrons provide an extra radiation burden to the patient [28]. For that comparison, we used readily available cortical astrocytes from neonatal rat origin. While sharing some traits with human astrocytes, rat astrocytes are generally smaller and structurally less complex and diverse. Therefore, direct comparison with the human glioblastoma cell lines under study should be evaluated with caution [29]. Our results revealed that U87 spheroids were the most sensitive to ^{64}Cu exposure, namely they presented the lowest viability and cell proliferation capacity and were the only ones having their growth compromised after exposure. On the other hand, spheroids derived from the U373 cell line were the ones that showed the most resistance to radionuclide exposure, only being significantly affected in their proliferative capacity when exposed to the highest dose. In the case of the non-tumoral cell line, even though the spheroids' viability was not severely affected upon ^{64}Cu exposure, the clonogenic capacity of spheroid-derived cells decreased, meaning that [^{64}Cu]$CuCl_2$ might also affect healthy tissues.

In the second phase of this work, we investigated potential mechanisms that could be involved in the response of spheroids to [^{64}Cu]$CuCl_2$. First, we carried out an uptake study in spheroids derived from all cell lines. The results obtained revealed an increased ^{64}Cu uptake in spheroids derived from the most sensitive cell line, while spheroids derived from the most resistant cell line had the lowest uptake. This further supports previous results and suggests that ^{64}Cu interaction with cells is related to increased cellular damage. Interestingly, the cell line with the highest uptake was not the one with the highest expression of CTR1, suggesting that there might be other key players involved in ^{64}Cu interaction with cells, such as the divalent metal transporter 1 (DMT1) also expressed in glioblastoma cell lines [14, 30, 31]. Even though CTR1 expression was lower in astrocytes, there was a high ^{64}Cu uptake by spheroids derived from this cell line. This could be explained by the role astrocytes play as regulators of copper homeostasis in the brain, being described as having increased uptake of Cu^+, mainly mediated by CTR1 and DTM1 [32].

Next, we tried to understand if the presence of cells with stem-like properties was correlated with spheroids' sensitivity to [^{64}Cu]$CuCl_2$, considering the role of CSCs in tumors' resistance [33]. In an attempt to identify these populations in glioblastoma spheroids, we selected two markers previously used to identify CSCs in this type of tumor, CD44 and CD117 [34, 35]. CD44 is a transmembrane receptor for glycosaminoglycan hyaluronan, found in healthy tissues but also in glioblastoma [34]. The interaction between CD44 and its ligand is reported to potentially mediate invasion, migration, and chemoresistance in several tumor types [36]. It is known that populations that express this marker are able to generate new tumors similar to the original one, in animal models, while populations that do not express CD44 cannot [34]. Furthermore, Breyer and colleagues have shown that CD44 inhibition affected glioblastoma progression in animal models [37]. In accordance with our results, CD44 expression in U87, U373, and T98G cells was close to 100% in previous studies [37–39], being larger in U373, followed by U87 and T98G cell lines [40]. The other CSC marker selected, CD117, also known as *c-kit*, the receptor tyrosine kinase for stem cell factor (SCF), is involved in neural stem cell survival and stimulation of cell growth in gliomas [41]. To our knowledge, only one study has detected the presence of $CD117^+$ cells in one of the three selected glioblastoma cell lines, U87. Specifically, authors detected a very small population in spheroids derived from this cell line (< 1%), similar to our findings [23]. Interestingly, the relative expression of CD117 ligand, SCF, was found to be considerably higher in T98G (measured by quantitative real-time RT-PCR) than in other glioblastoma cell lines [42], which could be related to a larger population of $CD117^+$ cells found in this study. As anticipated, cell lines having the highest stemness potential, T98G and U373, were the ones found to be less affected by [^{64}Cu]$CuCl_2$ exposure. Nonetheless, it is important to notice that CSC identification in tumors is still an evolving field and a consensus has not yet been established concerning which markers should be used to identify this cell population. Other cell surface markers, such as CD133, CD15, integrin α6, L1CAM, and A2B5 have been used to identify CSCs populations in glioblastoma [43]. In the future, a more accurate identification of stem-like cell populations in our glioblastoma spheroids is planned, as well as the identification of possible changes in these populations after [^{64}Cu]$CuCl_2$ exposure.

An important hallmark of ionizing radiation effects, like the one originated by ^{64}Cu decay, is ROS generation. ROS are highly reactive to several cellular macromolecules, such as DNA, being involved in genetic instability induction [44]. Moreover, Cu is a potent oxidant, further contributing to ROS generation [45]. Considering this, and aiming to further understand the damages caused by [^{64}Cu]$CuCl_2$, we assessed whether exposure to [^{64}Cu]$CuCl_2$ would lead to ROS generation in glioblastoma spheroids. Unlike what was theoretically expected, [^{64}Cu]$CuCl_2$ did not drastically increase ROS production in all cell lines. Instead, our results revealed that only exposure to higher doses led to ROS production, being this effect more pronounced in spheroids derived from U87. Bearing in mind that increased intracellular ROS

levels lead to apoptosis and senescence [46], the higher ROS generation in U87 spheroids might be one of the key mechanisms involved in the largest decrease of cellular viability and proliferative capacity observed after exposure to [^{64}Cu]$CuCl_2$.

Importantly, besides the mechanisms here evaluated, there might be other key factors playing a role in the response of glioblastoma spheroids to ^{64}Cu. For example, TP53 status might influence tumor cells' resistance to treatment. The TP53 gene encodes a transcription factor (p53) involved in processes such as cellular homeostasis, cell proliferation, and survival, among other functions. When the gene is not mutated, under stress conditions, p53 will promote cell cycle arrest, senescence, and apoptosis, avoiding damaged cell propagation [47]. Interestingly, the most sensitive cell line to ^{64}Cu exposure under the conditions of our study, U87, has been described as having a wild-type TP53, while the most resistant cell lines (U373 and T98G) present mutations in this gene [48]. Furthermore, other pathways might also be involved in the decrease of cellular viability and proliferation capacity of glioblastoma cells exposed to [^{64}Cu]$CuCl_2$, considering that cell lines with a mutant p53 also present sensitivity to the radiopharmaceutical. It has also been reported that the PTEN gene, involved in tumor suppression and regulation of cell growth and survival, is mutated in U373 and T98G, which might also be associated with an increased treatment resistance [49, 50]. In what concerns mutations in DNA repair genes, it is reported that the U87 cell line presents a larger number of single nucleotide variations in genes involved in homologous recombination and non-homologous end joining, important to repair DNA damages caused by radiation, in particular those caused by Auger Electrons [21, 50].

Overall, our results reinforce the potential of [^{64}Cu]$CuCl_2$ as a theranostic agent for glioblastoma, unveiling an increased therapeutic component that could help improve the prognosis of glioblastoma patients.

Conclusions

Altogether, our results further support the potential of [^{64}Cu]$CuCl_2$ as a theranostic agent for glioblastoma. Diagnosis of this type of tumor is possible when lower doses of the radionuclide are administered, while larger doses also cause damage to tumor cells. Nonetheless, there are still some questions that need to be further clarified. For instance, the impact of potential deleterious effects on non-tumoral tissues surrounding the tumors should be evaluated. Novel cellular models with increased robustness concerning the simulation of the brain/tumor environment are under development. These will allow to better investigate the glioblastoma biology inserted in a primitive human brain environment and would majorly increase the value of this type of research [51]. Additionally, it would be important to analyze ^{64}Cu distribution within the spheroids and, most relevantly, within the cells, as the range of Auger Electrons is very short and proximity to the nucleus is crucial to achieve a high therapeutic efficacy. Acknowledging these pitfalls, we plan on further developing new studies to elucidate ^{64}Cu distribution in spheroids, and also in more complex models that include co-culture with non-tumoral human brain cells. Afterward, animal studies should be conducted to better elucidate the translational potential of this simple radiopharmaceutical.

To our knowledge, this is the first study to explore the radiobiological effects of [^{64}Cu]$CuCl_2$ exposure in glioblastoma spheroids while also exploring the mechanisms responsible for the therapeutic responses observed. With this study, we reinforced the promising potential of ^{64}Cu as a theranostic agent with evidence that demonstrates its therapeutic purpose in advanced culture models with a high predictive value. Overall, the present study provides important insights toward a better understanding concerning the therapeutic effect and mode of action of ^{64}Cu in the context of glioblastoma.

Abbreviations

3D	Three-dimensional
64Cu-ATSM	Copper-64 labeled diacetyl-2,3-bis(N4-methyl-3-thiosemicarbazone)
ANOVA	One-way analysis of variance
APH	Acid phosphatase
CSC	Cancer stem cell
CTR1	Copper transporter 1
DCF	2,7-Dichlorodihydrofluorescein
DMEM	Dulbecco's modified eagle's medium
DMT1	Divalent metal transporter 1
ECM	Extracellular matrix
FACS	Fluorescence-activated cell sorting
FBS	Fetal bovine serum
H2DCF-DA	2,7-Dichlorodihydrofluorescein diacetate
HRP	Horseradish peroxidase
MEM	Minimum essential medium
PBS	Phosphate saline buffer
PCR	Polymerase chain reaction
PET	Positron emission tomography
RA	Rat astrocytes
ROS	Reactive oxygen species
RT	Radiation therapy
RT-PCR	Real time-polymerase chain reaction
S.E.M.	Standard error of the mean
TMZ	Temozolomide
WHO	World health organization

Supplementary Information

The online version contains supplementary material available at https://doi.org/10.1186/s13550-024-01084-8.

Additional file 1. Additional figures and analyses.

Acknowledgements
Not applicable.

Author contributions
JFG and FM contributed to the conception and design of the study. CIGP, ADMB, SB, and AF performed the experimental work. AJA, CLS, and FM contributed to reagents, materials, and analysis tools. CIGP and JFG wrote the first draft of the manuscript. All authors contributed to the manuscript revision and have read and approved the submitted version.

Funding
This work was supported by ICNAS PHARMA and by Fundação para a Ciência e a Tecnologia (FCT), Portugal, through the Grant UID/Multi/04349/2019 to C2TN and the PhD Fellowship 2020.07119.BD to CIGPinto. Funding received by iBB, from FCT (UIDB/04565/2020) and from Lisboa2020 (Project N. 007317), is also acknowledged.

Availability of data and materials
Data sharing is not applicable to this article as no datasets were generated or analyzed during the current study.

Declarations

Ethics approval and consent to participate
Not applicable.

Consent for publication
Not applicable.

Competing interests
The authors declare that they have no competing interests.

Received: 24 January 2024 Accepted: 21 February 2024
Published online: 07 March 2024

References

1. McKinnon C, Nandhabalan M, Murray SA, Plaha P. Glioblastoma: clinical presentation, diagnosis, and management. BMJ. 2021;374: n1560.
2. Aldape K, Zadeh G, Mansouri S, Reifenberger G, von Deimling A. Glioblastoma: pathology, molecular mechanisms and markers. Acta Neuropathol. 2015;129(6):829–48.
3. Monteiro AR, Hill R, Pilkington GJ, Madureira PA. The role of hypoxia in glioblastoma invasion. Cells. 2017;6(4):45.
4. Cilliers K, Muller CJF, Page BJ. Trace element concentration changes in brain tumors: a review. Anat Rec (Hoboken). 2020;303(5):1293–9.
5. Turecký L, Kalina P, Uhlíková E, Námerová S, Krizko J. Serum ceruloplasmin and copper levels in patients with primary brain tumors. Klin Wochenschr. 1984;62(4):187–9.
6. Mulware SJ. Comparative trace elemental analysis in cancerous and noncancerous human tissues using PIXE. J Biophys. 2013;2013: 192026.
7. Liou GY, Storz P. Reactive oxygen species in cancer. Free Radic Res. 2010;44(5):479–96.
8. Pasquali M, Martini P, Shahi A, Jalilian AR, Osso JA, Boschi A. Copper-64 based radiopharmaceuticals for brain tumors and hypoxia imaging. Q J Nucl Med Mol Imaging. 2020;64(4):371–81.
9. Ferrari C, Asabella AN, Villano C, Giacobbi B, Coccetti D, Panichelli P, et al. Copper-64 dichloride as theranostic agent for glioblastoma multiforme: a preclinical study. Biomed Res Int. 2015;2015: 129764.
10. Holland JP, Ferdani R, Anderson CJ, Lewis JS. Copper-64 Radiopharmaceuticals for Oncologic Imaging. PET Clin. 2009;4(1):49–67.
11. Chakravarty R, Chakraborty S, Dash A. 64Cu2+ Ions as PET probe: an emerging paradigm in molecular imaging of cancer. Mol Pharm. 2016;13(11):3601–12.
12. Gangemi V, Mignogna C, Guzzi G, Lavano A, Bongarzone S, Cascini GL, et al. Impact of [64Cu][Cu(ATSM)] PET/CT in the evaluation of hypoxia in a patient with Glioblastoma: a case report. BMC Cancer. 2019;19(1):1197.
13. Vaupel P. The role of hypoxia-induced factors in tumor progression. Oncologist. 2004;9(Suppl 5):10–7.
14. Pérès EA, Toutain J, Paty LP, Divoux D, Ibazizène M, Guillouet S, et al. ^{64}Cu-ATSM/6^{4C}u-Cl2 and their relationship to hypoxia in glioblastoma: a preclinical study. EJNMMI Res. 2019;9(1):114.
15. Pinto CIG, Bucar S, Alves V, Fonseca A, Abrunhosa AJ, da Silva CL, et al. Copper-64 chloride exhibits therapeutic potential in three-dimensional cellular models of prostate cancer. Front Mol Biosci. 2020;7: 609172.
16. Panichelli P, Villano C, Cistaro A, Bruno A, Barbato F, Piccardo A, et al. Imaging of brain tumors with copper-64 chloride: early experience and results. Cancer Biother Radiopharm. 2016;31(5):159–67.
17. Zanoni M, Piccinini F, Arienti C, Zamagni A, Santi S, Polico R, et al. 3D tumor spheroid models for in vitro therapeutic screening: a systematic approach to enhance the biological relevance of data obtained. Sci Rep. 2016;6:19103.
18. Alves F, Alves V, Carmo D, Neves S, et al. Production of copper-64 and gallium-68 with a medical cyclotron using liquid targets. Mod Phys Lett A. 2017;32(17):21.
19. Alves VH, Do Carmo SJC, Alves F, Abrunhosa AJ. Automated purification of radiometals produced by liquid targets. Instruments. 2018;2(3):17.
20. Chen W, Wong C, Vosburgh E, Levine AJ, Foran DJ, Xu EY. High-throughput image analysis of tumor spheroids: a user-friendly software application to measure the size of spheroids automatically and accurately. J Vis Exp. 2014;8(89):e51639.
21. Guerreiro JF, Alves V, Abrunhosa AJ, Paulo A, Gil OM, Mendes F. Radiobiological characterization of 64 $CuCl_2$ as a simple tool for prostate cancer theranostics. Molecules. 2018;23(11):2944.
22. Alexiou GA, Lazari D, Markopoulos G, Vartholomatos E, Hodaj E, Galani V, et al. Moschamine inhibits proliferation of glioblastoma cells via cell cycle arrest and apoptosis. Tumour Biol. 2017;39(5):1010428317705744.
23. Yilmazer A. Evaluation of cancer stemness in breast cancer and glioblastoma spheroids in vitro. 3 Biotech. 2018;8(9):390.
24. de Kruijff RM, van der Meer AJGM, Windmeijer CAA, Kouwenberg JJM, Morgenstern A, Bruchertseifer F, et al. The therapeutic potential of polymersomes loaded with 225Ac evaluated in 2D and 3D in vitro glioma models. Eur J Pharm Biopharm. 2018;127:85–91.
25. Däster S, Amatruda N, Calabrese D, Ivanek R, Turrini E, Droeser RA, et al. Induction of hypoxia and necrosis in multicellular tumor spheroids is associated with resistance to chemotherapy treatment. Oncotarget. 2017;8(1):1725–36.
26. Barisam M, Saidi MS, Kashaninejad N, Nguyen NT. Prediction of necrotic core and hypoxic zone of multicellular spheroids in a microbioreactor with a U-shaped barrier. Micromachines (Basel). 2018;9(3):94.
27. Mittler F, Obeïd P, Rulina AV, Haguet V, Gidrol X, Balakirev MY. High-content monitoring of drug effects in a 3D spheroid model. Front Oncol. 2017;7:293.
28. Catalogna G, Talarico C, Dattilo V, Gangemi V, Calabria F, D'Antona L, et al. The SGK1 kinase inhibitor si113 sensitizes theranostic effects of the 64$CuCl_2$ in human glioblastoma multiforme cells. Cell Physiol Biochem. 2017;43(1):108–19.
29. Oberheim NA, Takano T, Han X, He W, Lin JH, Wang F, et al. Uniquely hominid features of adult human astrocytes. J Neurosci. 2009;29(10):3276–87.
30. Miki K, Yagi M, Yoshimoto K, Kang D, Uchiumi T. Mitochondrial dysfunction and impaired growth of glioblastoma cell lines caused by antimicrobial agents inducing ferroptosis under glucose starvation. Oncogenesis. 2022;11(1):59.
31. Kim Y, Olivi L, Cheong JH, Maertens A, Bressler JP. Aluminum stimulates uptake of non-transferrin bound iron and transferrin bound iron in human glial cells. Toxicol Appl Pharmacol. 2007;220(3):349–56.
32. Scheiber IF, Dringen R. Astrocyte functions in the copper homeostasis of the brain. Neurochem Int. 2013;62(5):556–65.
33. Ishiguro T, Ohata H, Sato A, Yamawaki K, Enomoto T, Okamoto K. Tumor-derived spheroids: relevance to cancer stem cells and clinical applications. Cancer Sci. 2017;108(3):283–9.
34. Bradshaw A, Wickremsekera A, Tan ST, Peng L, Davis PF, Itinteang T. Cancer stem cell hierarchy in glioblastoma multiforme. Front Surg. 2016;3:21.
35. Kang MK, Kang SK. Tumorigenesis of chemotherapeutic drug-resistant cancer stem-like cells in brain glioma. Stem Cells Dev. 2007;16(5):837–47.
36. DeSouza LV, Matta A, Karim Z, Mukherjee J, Wang XS, Krakovska O, et al. Role of moesin in hyaluronan induced cell migration in glioblastoma multiforme. Mol Cancer. 2013;12:74.

37. Breyer R, Hussein S, Radu DL, Pütz KM, Gunia S, Hecker H, et al. Disruption of intracerebral progression of C6 rat glioblastoma by in vivo treatment with anti-CD44 monoclonal antibody. J Neurosurg. 2000;92(1):140–9.
38. Hartheimer JS, Park S, Rao SS, Kim Y. Targeting hyaluronan interactions for glioblastoma stem cell therapy. Cancer Microenviron. 2019;12(1):47–56.
39. Knüpfer MM, Poppenborg H, Van Gool S, Domula M, Wolff JE. Interferon-gamma inhibits proliferation and adhesion of T98G human malignant glioma cells in vitro. Klin Padiatr. 1997;209(4):271–4.
40. Hong X, Chedid K, Kalkanis SN. Glioblastoma cell line-derived spheres in serum-containing medium versus serum-free medium: a comparison of cancer stem cell properties. Int J Oncol. 2012;41(5):1693–700.
41. Sihto H, Tynninen O, Bützow R, Saarialho-Kere U, Joensuu H. Endothelial cell KIT expression in human tumours. J Pathol. 2007;211(4):481–8.
42. Sun L, Hui AM, Su Q, Vortmeyer A, Kotliarov Y, Pastorino S, et al. Neuronal and glioma-derived stem cell factor induces angiogenesis within the brain. Cancer Cell. 2006;9(4):287–300.
43. Lathia JD, Mack SC, Mulkearns-Hubert EE, Valentim CL, Rich JN. Cancer stem cells in glioblastoma. Genes Dev. 2015;29(12):1203–17.
44. Tominaga H, Kodama S, Matsuda N, Suzuki K, Watanabe M. Involvement of reactive oxygen species (ROS) in the induction of genetic instability by radiation. J Radiat Res. 2004;45(2):181–8.
45. Stefani C, Al-Eisawi Z, Jansson PJ, Kalinowski DS, Richardson DR. Identification of differential anti-neoplastic activity of copper bis(thiosemicarbazones) that is mediated by intracellular reactive oxygen species generation and lysosomal membrane permeabilization. J Inorg Biochem. 2015;152:20–37.
46. Moloney JN, Cotter TG. ROS signalling in the biology of cancer. Semin Cell Dev Biol. 2018;80:50–64.
47. Zhang Y, Dube C, Gibert M, Cruickshanks N, Wang B, Coughlan M, et al. The p53 pathway in glioblastoma. Cancers (Basel). 2018;10(9):297.
48. Ito H, Kanzawa T, Miyoshi T, Hirohata S, Kyo S, Iwamaru A, et al. Therapeutic efficacy of PUMA for malignant glioma cells regardless of p53 status. Hum Gene Ther. 2005;16(6):685–98.
49. Chen CY, Chen J, He L, Stiles BL. PTEN: tumor suppressor and metabolic regulator. Front Endocrinol (Lausanne). 2018;9:338.
50. Patil V, Pal J, Somasundaram K. Elucidating the cancer-specific genetic alteration spectrum of glioblastoma derived cell lines from whole exome and RNA sequencing. Oncotarget. 2015;6(41):43452–71.
51. Linkous A, Balamatsias D, Snuderl M, Edwards L, Miyaguchi K, Milner T, et al. Modeling patient-derived glioblastoma with cerebral organoids. Cell Rep. 2019;26(12):3203-11.e5.

Publisher's Note